

# Echoes from a Warped Dimension

Hooman Davoudiasl<sup>a\*</sup>

<sup>a</sup>Department of Physics, Brookhaven National Laboratory  
Upton, NY 11973, USA

The Randall-Sundrum (RS) model, based on a slice of warped 5D spacetime, was originally introduced to explain the apparent hierarchy between the scales of weak and gravitational interactions. Over the past decade, this model has been extended to provide a predictive theory of flavor, as well as to address various constraints from precision data. In this talk, we will present a brief review of the RS model and some of its extensions. A survey of some key signatures of realistic warped models and the experimental challenges they pose will be presented. We will also consider truncated warped scenarios that address smaller hierarchies and discuss why their discovery can have improved prospects, at the LHC.

## 1. Introduction

The following is based on an invited talk given by the author at The International Workshop on “Beyond the Standard Model Physics and LHC Signatures (BSM-LHC),” held at Northeastern University, Boston, MA, USA, June 2-4, 2009.

In the Standard Model (SM), electroweak symmetry breaking (EWSB) is achieved by the scalar Higgs doublet condensate  $\langle H \rangle = v$ . Given the quadratic sensitivity of Higgs mass to quantum corrections from an arbitrarily high mass scale  $M$ , one is faced with the question of why  $v \ll M$ . This is the general nature of what is referred to as the hierarchy problem. In particular, if  $M$  is near the Planck scale  $M_P \sim 10^{19}$  GeV, one is compelled to explain why  $v/M_P \sim 10^{-16}$ . Over the years many ideas have been advanced to explain the hierarchy, including strong dynamics, supersymmetry, and more recently extra dimensions. In this presentation, we will focus on a proposal for bridging the energy interval between a  $\mu$  g and 1 erg, through a warped extra dimension.

## 2. The Randall-Sundrum Model

Warped 5D models that we will examine here are generally based on the Randall-Sundrum (RS)

model [1], which is a slice of the  $\text{AdS}_5$  spacetime bounded by two 4D Minkowski walls at  $y = 0, \pi r_c$ , the UV and IR branes, respectively, along the fifth dimension. The RS metric is given by:

$$ds^2 = e^{-2ky} \eta_{\mu\nu} dx^\mu dx^\nu - dy^2, \quad (1)$$

where  $k$  is the curvature scale and is typically assumed to be somewhat smaller than the 5D fundamental scale  $M_5 \sim M_P$ . Physical mass scales get redshifted in this background as one goes from the UV brane to the IR brane. In particular, if the 5D Higgs condensate  $v_5 \sim k$  is IR-localized, the observed 4D value will be obtained from  $e^{-kr_c\pi} \langle H_5 \rangle$  with  $kr_c\pi \approx 36$ , hence resolving the hierarchy problem. We note that based on the AdS/CFT correspondence [2], there is a connection between certain 4D strong dynamical models and RS-type models [3], but we will not examine this subject any further here.

The most distinct signature of the original RS model is the appearance of a tower of spin-2 resonances, corresponding to the Kaluza-Klein (KK) states of the 5D graviton. These KK gravitons have masses and couplings governed by the TeV scale, and would couple to all SM fields universally. This gives rise to striking predictions for collider experiments [4]. Another aspect of the original RS phenomenology is related to the required stabilization of the size of the fifth dimension.

---

\*Work supported by the US Department of Energy under Grant Contract DE-AC02-98CH10886.

sion [5], whose quantum fluctuations gives rise to the *radion* scalar, with properties very similar to the SM Higgs [6]. The radion can mix with the Higgs, through a possible scalar-curvature coupling [7].

The Tevatron experiments have searched for the first graviton KK mode  $G^1$  in the original model and have not found a signal, resulting in the bounds presented in Figs.1 and 2, from the CDF ( $2.3 \text{ fb}^{-1}$ ) [8] and D0 ( $1 \text{ fb}^{-1}$ ) [9] experiments, respectively. Roughly speaking, the current data disfavors a  $G^1$  lighter than 900 GeV, for  $k/M_P = 0.1$ , at 95% confidence level.

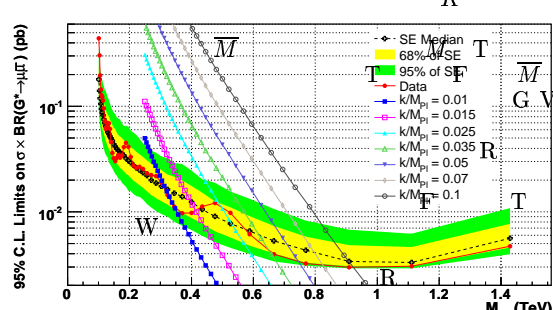


Figure 1. CDF limits, at 95% confidence level, on the product of cross section and di-muon branching ratio, for  $G^1$  in the original RS model. Theoretical cross sections, as well as the expected limits from simulated experiments (SE) are shown; from Ref. [8]

The LHC experiments ATLAS and CMS have examined their reach for  $G^1$  in the original RS model. With  $100 \text{ fb}^{-1}$  and  $k/M_P = 0.1$ , the ATLAS experiment [10] expects to be able to discover  $G^1$ , in the  $e^+e^-$  channel, up to a mass of 3.5 TeV, whereas the CMS reach is somewhat better (about 4 TeV), in the di-muon channel [11].

### 3. Warped Models of Hierarchy and Flavor

Although the original RS model provides an interesting resolution of the hierarchy problem

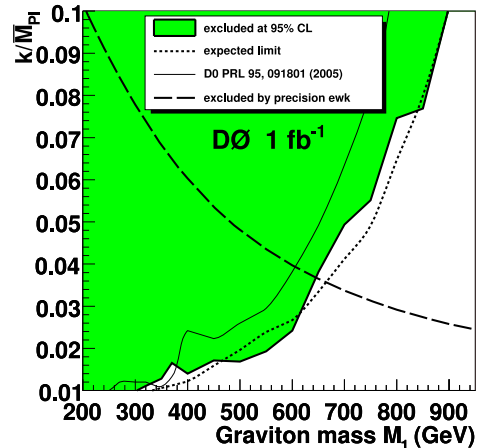


Figure 2. D0 bounds on  $G^1$ , using the  $e^+e^-$  and  $\gamma\gamma$  channels, from Ref. [9].

and had distinct testable predictions, it also gives rise to some phenomenological problems. For one thing, the model has a (quantum gravity) cutoff scale of  $\sim 1$  TeV, which is quite insufficient to suppress higher-dimensional operators that would cause deviations from precision EW or flavor data. Raising the cutoff scale, which is close to the KK scale of the IR brane, will introduce hierarchies that the model was meant to address. Also, the SM flavor structure still remains a mystery in this setup; while this is a short-coming shared by many models of hierarchy, it would be desirable to use the 5D bulk to address the flavor problem as well (as was done in the context of flat backgrounds [12]).

In fact, to address the hierarchy problem, it is sufficient to keep the Higgs near the IR brane and the rest of the SM can be allowed to reside in all five dimensions [13]. The gauge fields [14,15] and fermions [16] can be moved to the bulk, where 5D masses for the latter can give rise to a natural geometric mechanism, based on the overlap of 5D profiles with the IR-localized Higgs, to generate 4D fermion masses over a wide range of values. Here, the light fermions are localized near the UV brane, while heavy fermions are IR-localized. A

schematic representation of this setup is provided in Fig. 3. In addition to generating small masses,

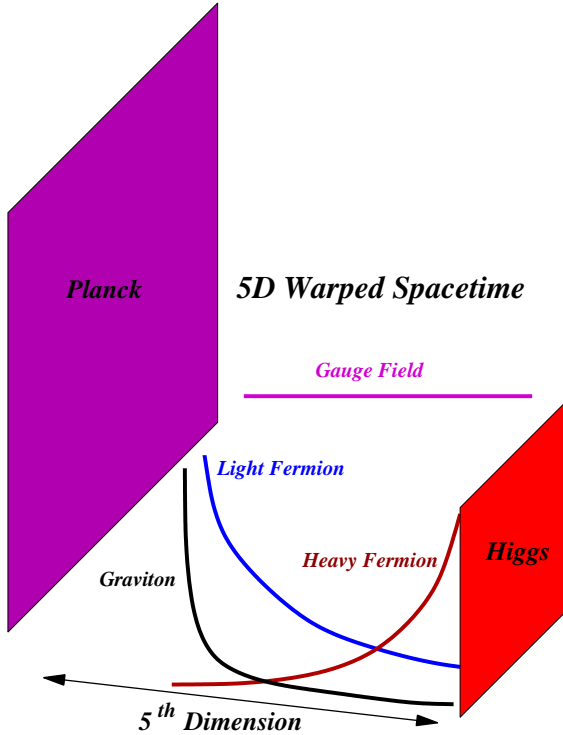


Figure 3. Schematic representation of a 5D warped model of hierarchy and flavor.

UV-localization of the light fermions also raises the effective cutoff scale for operators composed of these fields far above the TeV regime [17]. This feature provides for an efficient means of suppressing unwanted operators, such as those mediating flavor changing neutral current (FCNC) processes, related to the tightly constrained light flavors. Hence, 5D warped scenarios can also provide natural and predictive models of flavor, whose typical signals are expected to arise near the weak scale.

This simultaneous resolution of the hierarchy and flavor puzzles, within the extended warped models, comes at a price. That is, in these mod-

els, the new states become more elusive in collider experiments, and in particular, at the LHC. If we denote a generic SM gauge coupling by  $g_{SM}$ , the new couplings are roughly given as follows

- Gauge KK couplings:

- UV-brane (e.g.  $e, u$ ):  $\sim g/\sqrt{k\pi r_c}$
- IR-brane (e.g.  $H, t_R$ ):  $\sim g\sqrt{k\pi r_c}$

- Graviton KK couplings in  $\sim \text{TeV}^{-1}$  units:

- Light fermions:  $\sim$  Yukawa (overlap with the IR-localized graviton KK mode)
- IR-brane (e.g.  $H, t_R$ ):  $\sim 1$
- Gauge fields ( $g, \gamma$ ):  $\sim 1/(k\pi r_c)$  (volume suppressed).

We see that KK couplings to light SM fields, important for production (e.g. light quarks) and clean detection (e.g. the photon) at colliders, are suppressed in models that yield realistic 4D flavor patterns. Instead of the usual golden channels that are easy to detect, the KK modes most strongly couple to heavy SM fields, such as top quarks and the Higgs sector, including the longitudinal gauge fields  $W_L^\pm$  and  $Z_L$ , which require more complicated event reconstruction. In particular, the projections regarding the reach for signals of warped scenarios must be revised for models of hierarchy and flavor. However, before discussing the experimental prospects for the simplest warped models that also accommodate flavor, let us briefly review some of the relevant constraints from precision data and their implication for collider searches.

Even though fermion localization alleviates some of the problems with warped models a great deal, there are still some rather stringent experimental bounds that could push the masses of KK modes to scales high enough to render RS-type models unnatural from the point of view of the hierarchy and, in any case, inaccessible at the LHC. Of these, the constraints from oblique corrections can be brought under control by enlarging the bulk gauge group to  $G_c = SU(2)_L \times SU(2)_R \times U(1)_X$ , for gauge KK masses  $m_{KK} \gtrsim 3 \text{ TeV}$  [18], due to the custodial protection provided by  $G_c$ .

The gauge KK masses would be pushed to about 5 TeV or more, if we also include the constraints from the measured  $Zb\bar{b}$  coupling, unless we enhance the symmetry to  $G_c \times Z_2$  [19]. In addition, important bounds come from gluon KK exchange processes [20] contributing to the  $\epsilon_K$  parameter of  $K - \bar{K}$  mixing, the most severe of which comes from  $(V - A) \times (V + A)$  operators [21,22], that would require approximately  $m_{KK} \gtrsim 20$  TeV [23]. Without further tuning of parameters or extra flavor structure (see, for example, Ref. [24]) these bounds would not allow for observable KK states at the LHC. Nonetheless, in the following discussion we will assume that remedies are in place to address the flavor bounds and we will examine the discovery prospects in relation to constraints that are addressed by imposing  $G_c$  in the bulk.

#### 4. Realistic Bulk Flavor and LHC Signals

Next, we will give a brief summary of some of the works that have examined the discovery reach for 5D warped models with localized fermions that can explain the 4D SM flavor structure (for a more detailed survey of warped collider phenomenology and additional references, see, for example, Ref. [25]). These results typically apply to the simplest models, endowed with an IR-localized Higgs fields, and only consider the SM decay modes of the KK states. However, the width of these states can receive important contributions from light (compared to gauge KK masses) non-SM fermions that are present in models with custodial protection for the  $Zb\bar{b}$  coupling [26,27]. Unless otherwise specified, the LHC center of mass energy  $\sqrt{s} = 14$  TeV is assumed and the discovery reach is set by a  $5\sigma$  significance, in this section.

The KK gluon: The reach for the lightest KK gluon  $g^1$  was examined in Refs. [28,29]. Here, the production is from light quark initial states, which is suppressed as discussed before, and the dominant decay channel is into top quarks. The width of  $g^1$  is roughly given by  $m_{KK}/6$ . Apart from the requisite kinematic cuts, one could use the highly boosted top polarization as a handle on the signal. This is due to the preferential

coupling of  $g^1$  to one of the top chiralities, set by the different localization of the doublet and singlet states. The conclusion reached by both Refs. [28,29] indicate that with  $100 \text{ fb}^{-1}$ ,  $g^1$  up to masses of 3-4 TeV can be discovered at the LHC. Hence, at least from the point of view of non-flavor constraints [30], the LHC can probe a phenomenologically interesting regime for the mass of  $g^1$ .

The KK graviton: The graviton KK tower is a distinct signal of the RS background. Refs. [31, 32] revisited the LHC prospects for the discovery of the lightest graviton KK mode  $G^1$ . The only important initial states for the production of  $G^1$  are the gluons, with a volume-suppressed coupling. However,  $G^1$  has several important decay channels. Ref. [31] focused on the top decay channel and concluded that for top reconstruction efficiencies ranging over 1-100%, the reach for  $G^1$  can be 1.5-2 TeV, for  $100 \text{ fb}^{-1}$ . Here, the event reconstruction is more challenging, due to the collimated decay products of the top, given its high boost ( $E_t \sim 1$  TeV).

Ref. [32] considered the process  $gg \rightarrow G^1 \rightarrow Z_L Z_L \rightarrow 4\ell$ , with  $\ell = e, \mu$ , and found that with  $300 \text{ fb}^{-1}$ ,  $G^1$  up to a mass of about 2 TeV can be discovered at the LHC. The 4-lepton final state provides for a clean signal, but suffers from a small branching fraction. One may improve the signal by considering the hadronic final states of one of the  $Z$ 's. However, the high boost of the  $Z$  causes its dijet decay products to appear as a single jet, making  $Z + j$  the relevant SM background, which would overwhelm the signal. Here we note that the RS model predicts the mass of  $G^1$  to be  $3.83/2.45 \simeq 1.56$  times larger than the mass of the corresponding gauge KK state. Given our previous discussion of the precision bounds, we then expect the mass of  $G^1$  to be above 4 TeV, making its discovery a difficult challenge at the LHC.

The electroweak sector KK modes: Here, we assume that the bulk is endowed with a gauged  $SU(2)_L \times SU(2)_R \times U(1)_X$  symmetry. Given this gauge structure, at the first KK level, there are 3 neutral and 4 charged states, collectively denoted by  $Z'$  and  $W'$ , respectively.

Ref. [33] considered the reach for the  $Z'$ . The

main decay channels here are into  $t\bar{t}$ ,  $W_L W_L$ , and  $Z_L H$ . Due to the near degeneracy of the KK gluon and  $Z'$  masses, the top decay channel is dominated by the KK gluon “background.” This work concluded that in the  $Z' \rightarrow W_L^+ W_L^- \rightarrow \ell^+ \ell^- E_T$  channel, the reach for the  $Z'$  at the LHC is about 2 TeV, with  $100 \text{ fb}^{-1}$ . The use of the  $jj$  final state for the  $W$ ’s requires considering the large  $Wj$  SM background, since, as before, the dijet final state will appear as a single jet because of the boost of the parent particle. Ref. [27] considered the reach for the  $W'$ , where one might expect an improved reach due to (1) the more effective reconstruction of the  $WZ$  decay channel using clean purely leptonic final states, as there is only one neutrino in this case and (2) the  $W'$  decay into  $t\bar{b}$  is free from KK gluon contamination (unlike the case of the  $Z' \rightarrow t\bar{t}$ ). However, as it turns out, these advantages are offset by the smallness of the  $Z$  leptonic branching ratio and the challenge of distinguishing a highly boosted  $t$  from a  $b$  (making  $t\bar{t}$  a relevant reducible background to the  $t\bar{b}$  signal). Hence, by and large, Ref. [27] finds a reach for  $W'$  similar to that for  $Z'$  at the LHC.

Many of the above conclusions about the reach of the LHC for new resonances can be improved by having better control over the reducible backgrounds associated with the decays of highly boosted heavy SM states. We will not enter into a discussion of how more sophisticated analysis techniques may be employed to deal with such effects here. However, we mention that some recent works on top-jets and the substructure of high- $p_T$  jets can be found in Ref. [34] and Ref. [35], respectively. Another possibility to improve the identification of merged dijets can be from utilization of the electromagnetic (EM) calorimeter, with its finer segmentation, to look for the EM cores of the jets [36].

## 5. Models without an Elementary Higgs

Here, we will briefly summarize some key features of warped models that do not employ a Higgs field to achieve EWSB. We consider two classes: (1) warped Higgsless models and (2) fermion condensation models.

Warped Higgsless models: These models [38] (first introduced in the context of flat backgrounds [37]) achieve EWSB through a set of boundary conditions which basically allow one to remove certain zero modes from the low energy spectrum. Here, in the absence of a Higgs field, unitarity in longitudinal gauge boson scattering is restored via the exchange of KK modes. However, this introduces an inherent tension into such a setup: achieving a reliably calculable model up to energies  $E \gg 1$  TeV requires the KK modes to have  $m_{KK} \lesssim 1$  TeV, yet compliance with precision EW data typically demand  $m_{KK} \gtrsim 1$  TeV [39,40,41]. Also, these models do not provide a natural setting for obtaining a realistic 4D flavor structure [42].

Warped quark condensation: Given the enhanced coupling of KK gluons to IR-localized fermions, it is interesting to consider whether this coupling could lead to quark condensation and EWSB. In particular, for a sufficiently IR-localized quarks  $\psi_{L,R}$ , one ends up with a dimension-6 operator

$$\begin{aligned} & \frac{-g_1 g_2}{M_{KK}^2} (\bar{\psi}_{1L} \gamma_\mu T^a \psi_{1L}) (\bar{\psi}_{2R} \gamma^\mu T^a \psi_{2R}) = \\ & \frac{g_1 g_2}{M_{KK}^2} (\bar{\psi}_{1L} \psi_{2R}) (\bar{\psi}_{2R} \psi_{1L}) + \mathcal{O}(1/N_c), \end{aligned} \quad (2)$$

where  $N_c = 3$  is the number of colors. The structure of the leading operator results in the observed pattern of EWSB upon the condensation of  $\bar{\psi}_{1L} \psi_{2R}$ , through the exchange of KK gluons. A dynamical mass is also generated for the condensing quarks. In Ref. [43], the condensing fermions were assumed to belong to a fourth generation. Here, the fourth generation fermions have masses of several hundred GeV, and the KK modes have  $m_{KK} \gtrsim 1$  TeV. The composite Higgs is predicted to be very massive, with  $m_H \gtrsim 700$  GeV.

Ref. [44] considered a situation where the condensing quarks are the top quarks of the SM. In this model, an extra 5D quark with the quantum numbers of the right-handed top quark is needed to obtain realistic masses for the top quark. Here, assuming that various calculable and non-calculable contributions to the radion potential

are governed by the weak-scale, one finds that top-condensation sets the scale of KK masses at around 30 TeV. The composite Higgs comes out to have a mass  $m_H \sim 500$  GeV. The signatures of this setup are a color-charged quark with a mass of a few TeV and a very weakly coupled radion  $\phi$ , with inverse coupling scale of order 100 TeV and a light mass of  $m_\phi \lesssim 4$  GeV. Given that the radion can mediate FCNC processes among localized zero modes of 5D fermions [45], Ref. [46] considered possible constraints and signals associated with the decay process  $B \rightarrow X_s \phi$ , for  $m_\phi < m_B$ , in the warped top-condensation model of Ref. [44].

## 6. Warped Dark Matter

Here, we survey a few proposals for a dark matter candidate in the context of warped 5D models.

SO(10) GUT models: In Ref. [47], in order to suppress large violations of baryon number  $B$ , it was assumed to be a gauged 5D quantum number within a warped GUT model in which quarks and lepton come from different split multiplets. This leads to a good  $Z_3$  symmetry from a combination of  $SU(3)_c$  and  $B$ . Whereas the SM fields are not charged under  $Z_3$ , exotic KK particles (without zero modes) are. The lightest  $Z_3$ -charged particle (LZP), with the quantum numbers of a right-handed neutrino, is then stable in this setup and can be a good dark matter candidate.

Warped KK-parity models: If an extra dimension has symmetric boundaries, there is a discrete remnant of the original translation invariance that survives, referred to as KK-parity. However, obviously, the warped RS background does not allow for this feature. Hence, one could imagine manufacturing a symmetric warped background by gluing two identical copies of the RS geometry at either the UV or the IR boundary. This was considered in Ref. [48], where the first option was referred to as IR-UV-IR and the second one was referred to as UV-IR-UV. However, generally speaking, the IR-UV-IR setup has problems related to EW constraints and flavor, whereas the UV-IR-UV case suffers from gravitational (radion ghost) instabilities.

Minimal models: An example of such a model

is discussed in Ref. [49], where it was shown that a scalar odd under a  $Z_2$  symmetry can be a good TeV-scale dark matter.

## 7. Truncated RS Models

It was suggested, in Ref. [50], that some of the constraints on the RS model, rooted in the strong couplings of the KK modes to IR-brane-localized degrees of freedom, could be loosened if one addresses hierarchies less severe than that between  $M_P$  and the weak scale. That is, by reducing  $\sqrt{kr_c\pi}$ , the aforementioned KK couplings can become less strong, and, for example, tree-level contributions to the oblique  $T$  parameter can become much smaller [50]. It was noted that one could still use the RS background to construct natural models of flavor, irrespective of the Planck-weak hierarchy. In this case, one may still want to keep the UV scale at or above  $\sim 1000$  TeV (as a safe flavor scale); in Ref. [50] such truncated models were dubbed “Little Randall-Sundrum” (LRS) models. Hence if the IR-brane (KK physics) is characterized by scales of order 1 TeV we would have LRS models with  $kr_c\pi \gtrsim 6$ . However, the work of Ref. [51] has pointed out that the constraints from the  $\epsilon_K$  parameter require a somewhat larger UV scale, corresponding to  $kr_c\pi \gtrsim 7$ .

An interesting aspect of volume-truncation in LRS models, pointed out in Ref. [50], is the significant sensitivity of some KK properties to the truncation parameter

$$y = \frac{(kr_c)_{RS}}{(kr_c)_{LRS}}. \quad (3)$$

This can affect the experimental prospects for “Little” KK discovery at the LHC. To see this, let us consider the  $Z'$  production and decay. In the narrow width approximation, the signal  $S$  for  $f_1 \bar{f}_1 \rightarrow Z' \rightarrow f_2 \bar{f}_2$ , is proportional to the cross section

$$\sigma(f_1, f_2) \propto \Gamma_{Z'}^{f_1} \text{Br}_{f_2}, \quad (4)$$

where  $\Gamma_{Z'}^{f_1}$  is the partial width of  $Z'$  into  $f_1 \bar{f}_1$ , and  $\text{Br}_{f_2}$  is the  $Z'$  branching ratio into  $f_2 \bar{f}_2$ . The dominant decay modes, which control the total width  $\Gamma_{Z'}$  of the  $Z'$ , are IR-localized, with couplings that are enhanced by a factor of order

$\sqrt{kr_c\pi}$ . These dominant decay modes are also difficult to reconstruct and suffer from various reducible backgrounds, whereas the *clean* dilepton ( $\ell^+\ell^-$ ,  $\ell = e, \mu$ ) modes have small branching ratios  $\text{Br}_\ell$ , given their  $1/\sqrt{kr_c\pi}$  suppressed couplings to KK modes, due to UV-localization (similar to light quarks  $q$ ).

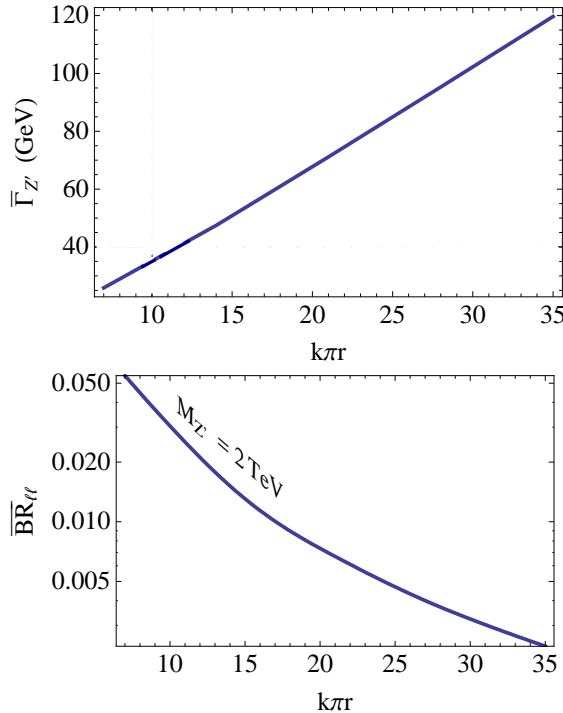


Figure 4. The width of a 2-TeV  $Z'$  (upper panel) and branching ratio into  $e$  or  $\mu$  pairs (lower panel), averaged over 3 neutral states, as a function of  $kr_c\pi$ ; from Ref. [52].

In warped models of flavor, we then have  $\Gamma_{Z'}^f \sim y$ , for  $f = q, \ell$ ,  $\Gamma_{Z'} \sim 1/y$ , and hence  $\text{Br}_\ell \sim y^2$ . Consequently, we expect that

$$S \propto \sigma(q, \ell) \sim y^3 \quad (5)$$

and the background under the resonance peak,

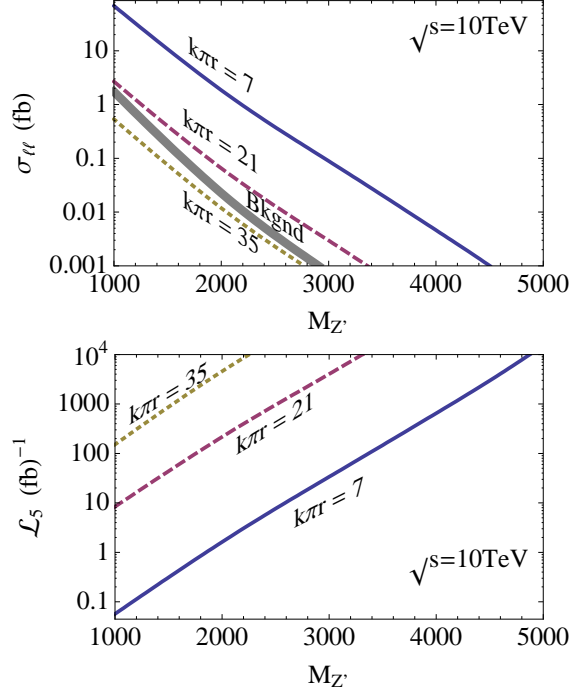


Figure 5. The cross section for  $pp \rightarrow Z' \rightarrow \ell^+\ell^-$  ( $\ell = e$  or  $\mu$ , not both) and the SM background (upper panel), after cuts [52], and the required integrated luminosity for a  $5\sigma$  signal with at least 3 events (lower panel), as a function of  $M_{Z'}$ . The LHC center of mass energy  $\sqrt{s} = 10$  TeV is assumed; from Ref. [52].

$B \propto \Gamma_{Z'} \sim 1/y$ . We hence find

$$S/B \sim y^4. \quad (6)$$

The remarkable enhancement in the signal size and quality for the clean dilepton decay modes of the  $Z'$  at the LHC, as suggested by the above simple analysis, points to an interesting possibility. That is, given the considerable sensitivity of important  $Z'$  branching ratios on the truncation parameter  $y$ , one may use TeV-scale data to probe the UV scale of the theory! Since the discovery of a KK-like resonance at the LHC does not necessarily point to a resolution of the Planck-weak hierarchy, such experimental handles on the UV-

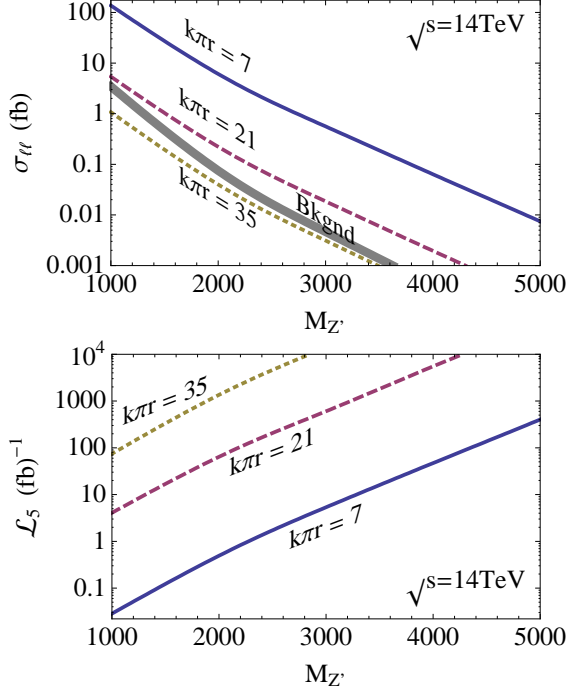


Figure 6. Same as Fig. 5, but for  $\sqrt{s} = 14$  TeV; from Ref. [52].

brane scale in the LRS models are quite valuable in deciphering the microscopic nature of the underlying theory.

A more quantitative examination of the effect of truncation on the LHC signals of warping is presented in Ref. [52] and we will focus on the  $Z'$  signals from this work. All the subsequent plots shown here are from Ref. [52]. The width of a 2-TeV  $Z'$  and its branching ratio into  $\ell^+\ell^-$  ( $\ell = e$  or  $\mu$ , not both) as a function of  $kr_c\pi$ , averaged over 3 states, are given in Fig. 4. These results confirm the expected behavior under truncation.

In Fig. 5, as a function of  $M_{Z'}$ , the cross section (upper panel) for  $pp \rightarrow Z' \rightarrow \ell^+\ell^-$  at the LHC with  $\sqrt{s} = 10$  TeV, after suitable cuts [52], and the required integrated luminosity for a  $5\sigma$  signal with at least 3 events (lower panel), for  $kr_c\pi = 7, 21, 35$ , are presented. These results suggest that, for  $kr_c\pi \approx 7$ , a 2-TeV Little  $Z'$

can be discovered in this clean decay channel, at  $\sqrt{s} = 10$  TeV, with only  $1 \text{ fb}^{-1}$ . This shows that phenomenologically interesting values of the UV brane scale, corresponding to  $M_5 \sim 10^4$  TeV, can be probed with *early* LHC data. The same quantities are shown for  $\sqrt{s} = 14$  TeV, as may be expected at later stages of the LHC running, in Fig. 6. Here, we can deduce that a 3-TeV Little  $Z'$  ( $kr_c\pi \approx 7$ ) can be discovered in the clean dilepton channel with only  $4 \text{ fb}^{-1}$  of integrated luminosity. This should be compared with the equivalent discovery reach requiring  $300 \text{ fb}^{-1}$ , in *any channel*, if  $M_5 \sim M_P$ , as in the original RS model. Hence, we see that truncation has a significant effect on the reach for warped KK modes and TeV information on such states can shed light on the UV scale of the 5D model.

## 8. Conclusions

Warped 5D models can provide a predictive framework to explain the hierarchy and flavor puzzles of the SM, and some of their variants can also provide good dark matter candidates. In these models the gauge and matter fermion content of the SM is placed in all 5D. Avoiding fine-tuning of parameters requires the introduction of extended 5D gauge symmetries, to protect precision EW observables from large corrections. With such protective symmetries, the masses of the KK modes can be in 2-3 TeV range, however flavor generally requires additional structure to avoid pushing KK modes to above  $\sim 10$  TeV. The warped models that provide realistic 4D flavor pose a challenge to LHC experiments, as they are characterized by suppressed couplings between the KK modes and light SM fields (important for production and detection).

However, if one relaxes the requirement of addressing the Planck-weak hierarchy, one could still obtain natural models of flavor, with fundamental 5D scales at or above  $\sim 10^4$  TeV. These truncated “Little Randall-Sundrum” models address the hierarchy between the high “flavor” scale and the weak scale (where the KK modes appear), but have much improved LHC discovery prospects. The sensitivity of the KK physics to truncation provides an opportunity for probing

reasonable values of the 5D scale of the underlying geometry, starting with early LHC data.

### Acknowledgments

We would like to thank the organizers of the 2009 BSM-LHC workshop for their invitation to give the talk upon which this writeup is based.

### REFERENCES

1. L. Randall and R. Sundrum, Phys. Rev. Lett. **83**, 3370 (1999) [arXiv:hep-ph/9905221].
2. J. M. Maldacena, Adv. Theor. Math. Phys. **2**, 231 (1998) [Int. J. Theor. Phys. **38**, 1113 (1999)] [arXiv:hep-th/9711200].
3. N. Arkani-Hamed, M. Poratti and L. Randall, JHEP **0108**, 017 (2001) [arXiv:hep-th/0012148]; R. Rattazzi and A. Zaffaroni, JHEP **0104**, 021 (2001) [arXiv:hep-th/0012248].
4. H. Davoudiasl, J. L. Hewett and T. G. Rizzo, Phys. Rev. Lett. **84**, 2080 (2000) [arXiv:hep-ph/9909255].
5. W. D. Goldberger and M. B. Wise, Phys. Rev. Lett. **83**, 4922 (1999) [arXiv:hep-ph/9907447].
6. W. D. Goldberger and M. B. Wise, Phys. Lett. B **475**, 275 (2000) [arXiv:hep-ph/9911457].
7. C. Csaki, M. L. Graesser and G. D. Kribs, Phys. Rev. D **63**, 065002 (2001) [arXiv:hep-th/0008151].
8. T. Aaltonen *et al.* [CDF Collaboration], Phys. Rev. Lett. **102**, 091805 (2009) [arXiv:0811.0053 [hep-ex]].
9. V. M. Abazov *et al.* [D0 Collaboration], Phys. Rev. Lett. **100**, 091802 (2008) [arXiv:0710.3338 [hep-ex]].
10. B. C. Allanach, K. Odagiri, M. J. Palmer, M. A. Parker, A. Sabetfakhri and B. R. Webber, JHEP **0212**, 039 (2002) [arXiv:hep-ph/0211205].
11. I. Belotelov *et al.*, CERN-CMS-NOTE-2006-104.
12. N. Arkani-Hamed and M. Schmaltz, Phys. Rev. D **61**, 033005 (2000) [arXiv:hep-ph/9903417].
13. W. D. Goldberger and M. B. Wise, Phys. Rev. D **60**, 107505 (1999) [arXiv:hep-ph/9907218].
14. H. Davoudiasl, J. L. Hewett and T. G. Rizzo, Phys. Lett. B **473**, 43 (2000) [arXiv:hep-ph/9911262].
15. A. Pomarol, Phys. Lett. B **486**, 153 (2000) [arXiv:hep-ph/9911294].
16. Y. Grossman and M. Neubert, Phys. Lett. B **474**, 361 (2000) [arXiv:hep-ph/9912408].
17. T. Gherghetta and A. Pomarol, Nucl. Phys. B **586**, 141 (2000) [arXiv:hep-ph/0003129].
18. K. Agashe, A. Delgado, M. J. May and R. Sundrum, JHEP **0308**, 050 (2003) [arXiv:hep-ph/0308036].
19. K. Agashe, R. Contino, L. Da Rold and A. Pomarol, Phys. Lett. B **641**, 62 (2006) [arXiv:hep-ph/0605341].
20. K. Agashe, G. Perez and A. Soni, Phys. Rev. D **71**, 016002 (2005) [arXiv:hep-ph/0408134].
21. G. Beall, M. Bander and A. Soni, Phys. Rev. Lett. **48**, 848 (1982).
22. M. Bona *et al.* [UTfit Collaboration], JHEP **0803**, 049 (2008) [arXiv:0707.0636 [hep-ph]].
23. C. Csaki, A. Falkowski and A. Weiler, JHEP **0809**, 008 (2008) [arXiv:0804.1954 [hep-ph]].
24. A. L. Fitzpatrick, L. Randall and G. Perez, Phys. Rev. Lett. **100**, 171604 (2008).
25. H. Davoudiasl, S. Gopalakrishna, E. Ponton and J. Santiago, arXiv:0908.1968 [hep-ph].
26. M. Carena, A. D. Medina, B. Panes, N. R. Shah and C. E. M. Wagner, Phys. Rev. D **77**, 076003 (2008) [arXiv:0712.0095 [hep-ph]].
27. K. Agashe, S. Gopalakrishna, T. Han, G. Y. Huang and A. Soni, arXiv:0810.1497 [hep-ph].
28. K. Agashe, A. Belyaev, T. Krupovnickas, G. Perez and J. Virzi, Phys. Rev. D **77**, 015003 (2008) [arXiv:hep-ph/0612015].
29. B. Lillie, L. Randall and L. T. Wang, JHEP **0709**, 074 (2007) [arXiv:hep-ph/0701166].
30. M. S. Carena, E. Ponton, J. Santiago and C. E. M. Wagner, Phys. Rev. D **76**, 035006 (2007) [arXiv:hep-ph/0701055].
31. A. L. Fitzpatrick, J. Kaplan, L. Randall and L. T. Wang, JHEP **0709**, 013 (2007) [arXiv:hep-ph/0701150].
32. K. Agashe, H. Davoudiasl, G. Perez and

A. Soni, Phys. Rev. D **76**, 036006 (2007) [arXiv:hep-ph/0701186].

33. K. Agashe *et al.*, Phys. Rev. D **76**, 115015 (2007) [arXiv:0709.0007 [hep-ph]].

34. J. Thaler and L. T. Wang, JHEP **0807**, 092 (2008) [arXiv:0806.0023 [hep-ph]]; D. E. Kaplan, K. Rehermann, M. D. Schwartz and B. Tweedie, Phys. Rev. Lett. **101**, 142001 (2008) [arXiv:0806.0848 [hep-ph]]; L. G. Almeida, S. J. Lee, G. Perez, I. Sung and J. Virzi, Phys. Rev. D **79**, 074012 (2009) [arXiv:0810.0934 [hep-ph]].

35. L. G. Almeida, S. J. Lee, G. Perez, G. Sterman, I. Sung and J. Virzi, Phys. Rev. D **79**, 074017 (2009) [arXiv:0807.0234 [hep-ph]].

36. Frank Paige, private communication.

37. C. Csaki, C. Grojean, H. Murayama, L. Pilo and J. Terning, Phys. Rev. D **69**, 055006 (2004) [arXiv:hep-ph/0305237].

38. C. Csaki, C. Grojean, L. Pilo and J. Terning, Phys. Rev. Lett. **92**, 101802 (2004) [arXiv:hep-ph/0308038].

39. Y. Nomura, JHEP **0311**, 050 (2003) [arXiv:hep-ph/0309189].

40. R. Barbieri, A. Pomarol and R. Rattazzi, Phys. Lett. B **591**, 141 (2004) [arXiv:hep-ph/0310285].

41. H. Davoudiasl, J. L. Hewett, B. Lillie and T. G. Rizzo, Phys. Rev. D **70**, 015006 (2004) [arXiv:hep-ph/0312193].

42. C. Csaki, C. Grojean, J. Hubisz, Y. Shirman and J. Terning, Phys. Rev. D **70**, 015012 (2004) [arXiv:hep-ph/0310355].

43. G. Burdman and L. Da Rold, JHEP **0712**, 086 (2007) [arXiv:0710.0623 [hep-ph]].

44. Y. Bai, M. Carena and E. Ponton, arXiv:0809.1658 [hep-ph].

45. A. Azatov, M. Toharia and L. Zhu, Phys. Rev. D **80**, 031701 (2009) [arXiv:0812.2489 [hep-ph]].

46. H. Davoudiasl and E. Ponton, arXiv:0903.3410 [hep-ph].

47. K. Agashe and G. Servant, Phys. Rev. Lett. **93**, 231805 (2004) [arXiv:hep-ph/0403143].

48. K. Agashe, A. Falkowski, I. Low and G. Servant, JHEP **0804**, 027 (2008) [arXiv:0712.2455 [hep-ph]].

49. E. Ponton and L. Randall, JHEP **0904**, 080 (2009) [arXiv:0811.1029 [hep-ph]].

50. H. Davoudiasl, G. Perez and A. Soni, Phys. Lett. B **665**, 67 (2008) [arXiv:0802.0203 [hep-ph]].

51. M. Bauer, S. Casagrande, L. Grunder, U. Haisch and M. Neubert, arXiv:0811.3678 [hep-ph].

52. H. Davoudiasl, S. Gopalakrishna and A. Soni, arXiv:0908.1131 [hep-ph].

